Technobius Physics, 2024, 2(1), 0007, DOI: https://doi.org/10.54355/tbusphys/2.1.2024.0007

Technobius Physics

https://technobiusphysics.kz/

e-ISSN 3007-0147

Article

Comparative analysis of copper X-radiation intensity with LiF and KBr crystals

Dias Sagatov*

Laboratory of Energy Storage Systems, National Laboratory Astana, 53 Kabanbay ave., Astana, Kazakhstan
*Correspondence: dias.sagatov@list.ru

Abstract. The intensity of copper X-radiation has been scrutinized as a function of the Bragg angle, employing both LiF and KBr crystals. X-ray intensity spectra were recorded for Cu as a function of Bragg angle using LiF, KBr single crystals using a PHYWE X-Ray Expert Unit (35 kV, 1 mA) with an X-ray goniometer, Plug-in Cu X-ray tube and a 2.2 mm diameter aperture tube. The scanning range was chosen to be 4°-55° for LiF and 3°-75° for KBr. The resultant spectra furnish a comprehensive portrayal of the variation in X-ray emission intensity relative to alterations in the Bragg angle. This investigation contributes to our comprehension of crystallographic phenomena and underscores the efficacy of diverse crystalline materials in X-ray diffraction studies. Precise determinations of the energy levels for characteristic copper X-ray lines have been obtained, revealing E ($K\beta$) = 8868.374 ± 30.474 eV and ($K\alpha$) = 8026.349 ± 31.634 eV. These findings accentuate the significance of X-ray spectroscopy in delineating the elemental composition and structural attributes of materials, while also affirming the role of theoretical predictions in elucidating experimental observations.
Keywords: X-ray spectroscopy, Bragg angle, copper X-radiation, crystallographic phenomena, energy determination.

1. Introduction

Undoubtedly, X-ray diffraction stands as the cornerstone of solid-state physics and chemistry, representing the most pivotal and extensively utilized technique within these fields. X-ray generation stemming from collisions between protons or light ions and atoms stands as a pivotal area of investigation for understanding inner-shell ionization mechanisms. This subject has undergone extensive examination from experimental and theoretical standpoints over recent decades, yielding significant insights. Notably, extensive collections of experimental X-ray cross-section data have been assembled for K and L shells ionized by protons and helium ions, enabling meticulous comparisons with established theoretical models [1–5].

When high-energy electrons collide with the metallic anode within an X-ray tube, they generate X-rays characterized by a continuous energy spectrum. Embedded within this continuum are specific X-ray lines, known as characteristic X-ray lines, which remain independent of the anode voltage and are unique to the composition of the anode material. These lines originate from the ionization of an anode atom's K shell when struck by an electron. Subsequently, the resulting vacancy within the shell is filled by an electron transitioning from a higher energy level. The energy liberated during this de-excitation process manifests as an X-ray emission distinct to the anode atom.

X-ray spectroscopy serves as a pivotal tool in the realm of material characterization, offering unparalleled insights into the elemental composition and structural properties of diverse substances. The analysis of X-ray emission intensity as a function of the Bragg angle, facilitated by crystals such as LiF and KBr, constitutes a fundamental aspect of X-ray diffraction studies [6–8]. This investigation aims to elucidate the intricate relationship between Bragg angle variations and copper X-radiation intensity, thereby advancing our understanding of crystallographic phenomena. Additionally, precise determinations of energy levels for characteristic copper X-ray lines further underscore the utility of X-ray spectroscopy in unraveling the intricacies of material properties. By combining experimental

observations with theoretical predictions, this study endeavors to provide a comprehensive framework for interpreting X-ray diffraction data and exploring the structural characteristics of materials at the atomic level [9-10].

The aim of this article is to explore and elucidate the phenomenon of X-ray production resulting from collisions between protons or other light ions and atoms. By examining this process from both experimental and theoretical perspectives, the article seeks to enhance our understanding of inner-shell ionization mechanisms. Additionally, it aims to provide detailed comparisons between experimental X-ray cross-section data and existing theoretical models, thereby advancing the current understanding of X-ray generation in such collisions.

2. Methods

The X-ray intensity spectra have been recorded for copper as a function of Bragg angle using mounted LiF, KBr single crystals. X-ray spectra were recorded using a PHYWE X-Ray Expert Unit (35 kV, 1mA) with X-ray goniometer, X-ray Plug-in Cu tube and Diaphragm tube with the diameter of 2.2 mm (Figure 1). An X-ray tube with a copper anode generates X-radiation that is selected with the aid of a mounted crystal (LiF and KBr) as a function of the Bragg angle. A Geiger-Muller counter tube with the size of 15 mm measures the intensity of the radiation. The glancing angles of the characteristic X-ray lines are then used to determine the energy. The spectra were scanned in the range 4°-55° for LiF and 3°-75° for KBr with the gate time of 2 s and angle step width 0.1° using a XR 4.0 Software. The goniometer has been programmed for automatic calibration to obtain accurate reflection angles.

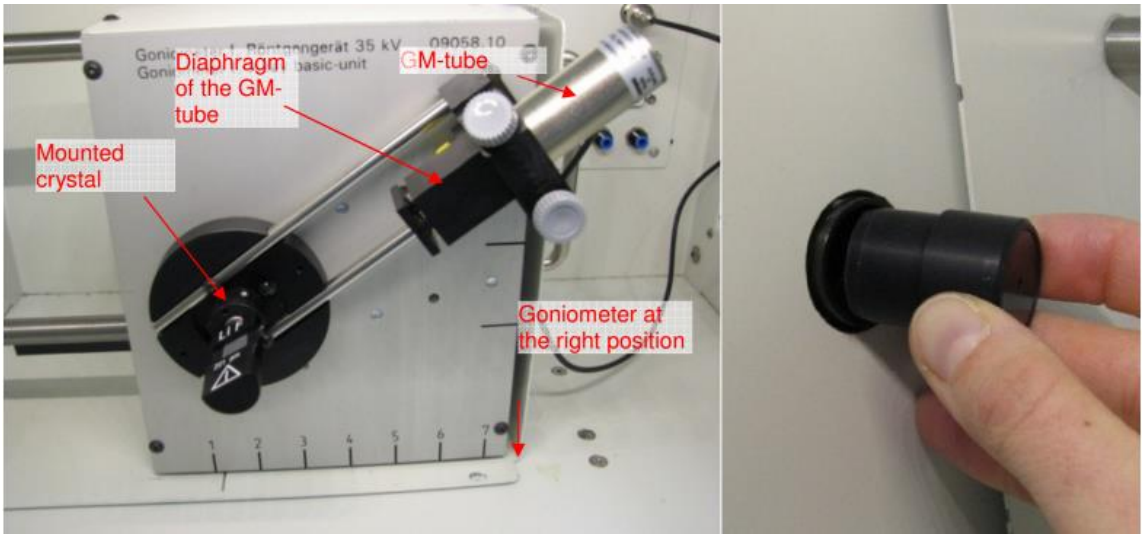

Figure 1 – Installation of X-ray goniometer and Geiger-Muller counter tube

Set of mounted LiF and KBr crystals were purchased at the PHYWE Company with crystallographic orientation of 100. All crystals were 1 mm thick and had a usable surface area of 10 x 12 mm. The lattice spacing was 201.4 pm for the LiF crystal and 329 pm for KBr. There are also differences in the treated surface of the crystals, LiF has undergone polishing while KBr has not. All crystals used are assumed to be pure without any impurities.

3. Results and Discussion

As is known, when high-energy electrons hit the metal anode of an X-ray tube, X-rays with a continuum energy distribution are produced. We have analyzed polychromatic X-rays using LiF and KBr crystals (Figure 2–3).

Figure 2 presents copper X-ray intensity specrtra recorded in range of 4°-55° for LiF crystals. The curve has a distinct peaks overlaying the continuous spectrum of the bremsstrahlung. The positions of these peaks remain consistent regardless of fluctuations in the anode voltage, suggesting their characteristic nature as copper lines. The initial set of lines corresponds to the first order of diffraction (n = 1), whereas the subsequent set corresponds to n = 2. This arises from the condition where X-rays of wavelength λ approach the crystal at an angle v, leading to constructive interference post-scattering only when the path difference δ between the partial waves reflected from the lattice planes equals one or more wavelengths.

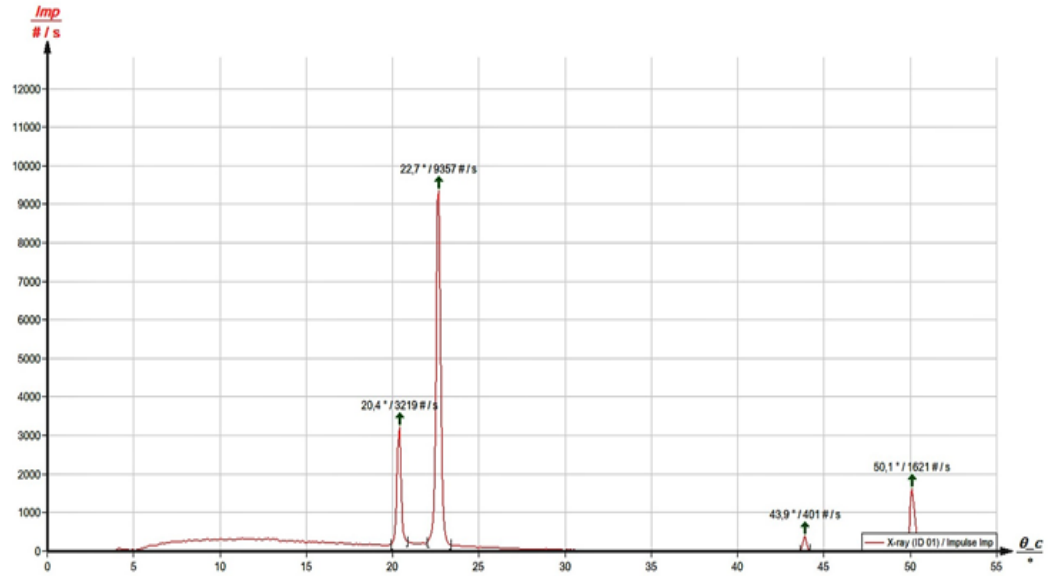

Figure 2 – Copper X-ray intensity as a function of the angle of incidence with LiF crystal as a Bragg analyzer

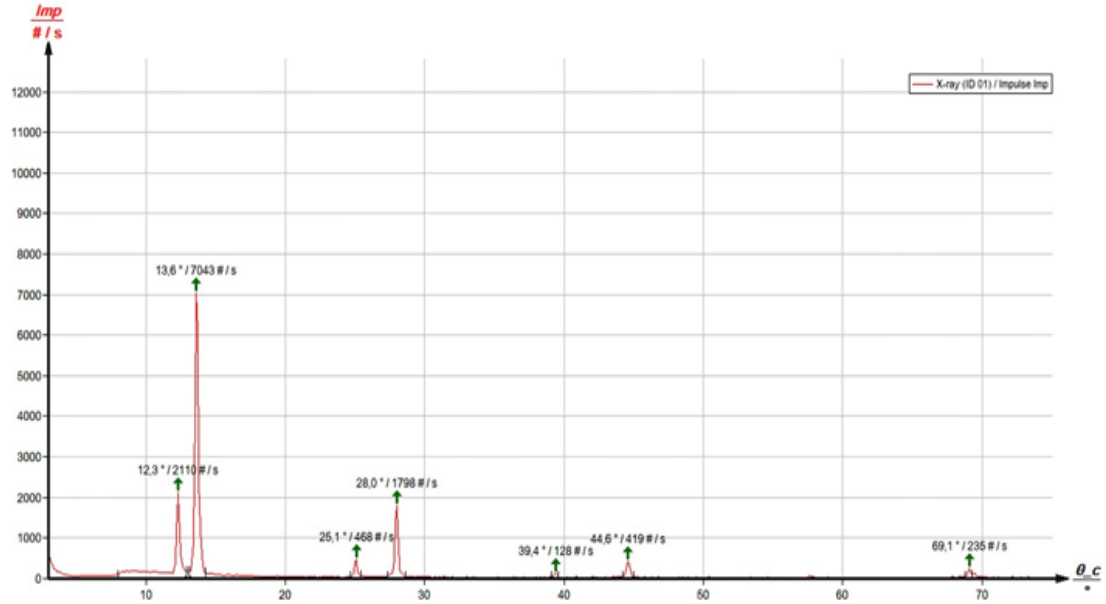

Figure 3 – Copper X-ray intensity as a function of the angle of incidence with KBr crystal as a Bragg analyzer

Substituting the LiF crystal with a KBr crystal in the examination of the copper X-ray spectrum permits Bragg scatterings up to the fourth order of diffraction (n = 4) as illustrated in Figure 3. The supplementary patterns observed beyond those depicted in Figure 3 stem from the increased

lattice constant of the KBr crystal. The maximums recorded during X-ray irradiation in range of 3°-75° also refer to characteristic copper peaks.

The bremsstrahlung spectrum depicted in Figure 3 exhibits a significant decrease in intensity towards smaller angles, notably at 8.0° and 16.3°. This decline aligns precisely with the theoretically anticipated bromide K absorption edge (E_K = 13.474 keV) within the first and second orders of diffraction. However, the potassium, lithium, and fluorine K absorption edges remain undetectable due to the bremsstrahlung spectrum's insufficient intensity within these energy ranges.

In pursuit of discerning the energy values associated with the characteristic X-ray emission of copper, and subsequently conducting a comparative analysis with those determined through the corresponding energy level diagram, our approach involved the utilization of the dataset delineated in Table 1.

Table 1 – Obtained experimental data of alkali halide crystals

Crystals	Initiation, deg	Maximum, deg	Shift, deg	Height, no/s	Area, no/s^2
LiF	19.8	20.5	20.8	3220.0	1022.0
	22.1	22.8	23.2	9355.1	3123.4
	43.7	44.0	44.1	405.11	102.5
	49.7	50.2	50.5	1624.2	567.8
KBr	8.0	12.4	12.8	2110.3	1302.1
	13.2	13.3	14.2	7043.4	2209.2
	24.9	25.2	25.2	468.12	141.25
	27.2	28.1	28.4	1798.3	554.62
	39.3	39.5	39.3	128.21	39.83
	44.1	44.7	45.1	419.01	149.14
	68.6	69.2	69.2	235.31	71.23

Table 2 – The calculated energy values pertaining to the characteristic copper X-ray lines

Crystals	Level	v/°, deg	Line	$E_{exp,}$ keV
LiF	n = 1	20.3	K_β	8831.201
		22.6	K_α	7975.936
	n = 2	43.8	K_β	8877.862
		50.2	K_α	8024.243
KBr	n = 1	12.2	K_β	8844.761
		13.7	K_α	8013.031
	n = 2	25.2	K_β	8883.512
		28.1	K_α	8025.795
	n = 3	39.5	K_β	8904.498
		44.7	K_α	8051.154
	n = 4		K_β	
		69.3	K_α	8067.587

4. Conclusions

The intensity of copper X-radiation has been analyzed as a function of the Bragg angle, utilizing both LiF and KBr crystals. The observed spectra offer a comprehensive depiction of how the intensity of X-ray emissions varies with changes in the Bragg angle, thereby contributing to our understanding of crystallographic phenomena and the utility of different crystalline materials in X-ray diffraction studies.

Furthermore, the calculated energy values for the characteristic copper X-ray lines yield E ($K\beta$) = 8868.374 ± 30.474 eV and ($K\alpha$) = 8026.349 ± 31.634 eV, providing precise determinations

for these energy levels. These findings underscore the utility of X-ray spectroscopy in elucidating the elemental composition and structural characteristics of materials, while also highlighting the efficacy of theoretical predictions in interpreting experimental observations.

References

1. Fitted empirical reference cross sections for K-shell ionization by protons / H. Paul, J. Sacher // Atomic Data and Nuclear Data Tables. — 1989. — Vol. 42, No. 1. — P. 105–156. https://doi.org/10.1016/0092-640X(89)90033-8
2. Cross Sections for K-shell X-ray Production by Hydrogen and Helium Ions in Elements from Beryllium to Uranium / G. Lapicki // Journal of Physical and Chemical Reference Data. — 1989. — Vol. 18, No. 1. — P. 111–218. https://doi.org/10.1063/1.555838
3. Present status of the experimental L-shell ionization cross sections for light ion impact / I. Orlic // Nuclear Instruments and Methods in Physics Research Section B: Beam Interactions with Materials and Atoms. — 1994. — Vol. 87, No. 1. — P. 285–292. https://doi.org/10.1016/0168-583X(94)95274-4
4. Energy-loss effect in inner-shell Coulomb ionization by heavy charged particles / W. Brandt, G. Lapicki // Physical Review A. — 1981. — Vol. 23, No. 4. — P. 1717–1729. https://doi.org/10.1103/PhysRevA.23.1717
5. Cooper-minimum-type structure in proton-induced L1- and L3- subshell x-ray line intensities of Pd measured with high-resolution x-ray spectroscopy / M. Kavčič, Ž. Šmit // Physical Review A. — 2009. — Vol. 79, No. 5. — P. 052708. https://doi.org/10.1103/PhysRevA.79.052708
6. Specific conductance of the molten LiF-KCl and LiF-KBr systems / C. Xu, G. Liu, N. Chen // Jinshu Xuebao/Acta Metallurgica Sinica. — 1984. — Vol. 20, No. 5. — P. b320–b322.
7. 3D Atomic Arrangement at Functional Interfaces Inside Nanoparticles by Resonant High-Energy X-ray Diffraction / V. Petkov, B. Prasai, S. Shastri, T.-Y. Chen // ACS Applied Materials and Interfaces. — 2015. — Vol. 7, No. 41. — P. 23265–23277. https://doi.org/10.1021/acsami.5b07391
8. Measurement of Fall Rate and Analysis of Atmospheric Falling Dust in Duhok Governorate of Iraq by Using Atomic Absorption Spectrometry and X-ray Diffraction / B.H. Mahdi // Journal of Physics: Conference Series. — 2021. — Vol. 1829. — P. 012001. https://doi.org/10.1088/1742-6596/1829/1/012001
9. Inhomogeneous thermal expansion of metallic glasses in atomic-scale studied by in-situ synchrotron X-ray diffraction / A.H. Taghvaei, H. Shakur Shahabi, J. Bednarčik, J. Eckert // Journal of Applied Physics. — 2015. — Vol. 117, No. 4. — P. 187–195. https://doi.org/10.1063/1.4906552
10. Study of the structural quality of heteroepitaxial silicon-on-sapphire structures by high-resolution X-ray diffraction, X-ray reflectivity, and electron microscopy / A.E. Blagov, A.L. Vasiliev, A.S. Golubeva, I.A. Ivanov, O.A. Kondratev, Yu.V. Pisarevsky, M.Yu. Presnyakov, P.A. Prosekov, A.Yu. Seregin // Crystallography Reports. — 2014. — Vol. 59, No. 3. — P. 315–322. https://doi.org/10.1134/S1063774514030043

Information about author:
Dias Sagatov – Research Assistant, Laboratory of Energy Storage Systems, National Laboratory Astana, 53 Kabanbay ave., Astana, Kazakhstan, dias.sagatov@list.ru

Author Contributions:
Dias Sagatov – concept, methodology, resources, data collection, testing, modeling, analysis, visualization, interpretation, drafting, editing, funding acquisition.

Conflict of Interest: The authors declare no conflict of interest.

Use of Artificial Intelligence (AI): The authors declare that AI was not used.

Received: 03.10.2023
Revised: 23.10.2023
Accepted: 13.11.2023
Published: 16.01.2024